Oscillatory dynamics of the Belousov–Zhabotinsky system in the presence of a self-assembling nonionic polymer. Role of the reactants concentration

Luciana Sciascia,† Federico Rossi,‡ Carmelo Sbriziolo, Maria Liria Turco Liveri* and Rosario Varsalona

Received 12th February 2010, Accepted 14th June 2010
DOI: 10.1039/c003033c

In the present study, the role played by the reactants concentration on the nonlinear response of a Belousov–Zhabotinsky (BZ) system to the addition of a self-assembling non-ionic polymer, poly(ethylene glycol) (PEG), has been assessed. The oscillatory parameters are influenced to an extent that significantly depends on the concentration of both the polymer and the Belousov–Zhabotinsky components. The effects obtained were attributed to the reaction among some of the BZ key species and the backbone and the alcoholic functional groups of the polymer, both in its monomeric and aggregated forms.

Support to the proposed perturbation mechanism has been provided by performing numerical simulations with the MBM model and by characterizing the physicochemical behavior of the PEG aqueous solution by means of viscosimetric and spectrofluorimetric measurements.

Introduction

Nonlinear dynamics (NLD) is nowadays one of the most fascinating and promising topics in scientific research. In fact, the phenomena exhibited by many nonlinear systems seem to be present in a ubiquitous way in many fields such as physics, chemistry, biology, social sciences, *etc*. and have therefore stimulated the interaction and cross-linking between such different points of view and areas of interest.

Among the NLD phenomena present in chemical systems, the Belousov–Zhabotinsky reaction (BZ)[1,2] is undoubtedly one of the most interesting and most studied.[3] In its classical form it consists in the catalyzed oxidation of an organic substrate, such as malonic acid, by bromate in acidic solution. Typical catalysts are the Ce(IV)/Ce(III) or Ferrin/Ferroin redox couples. The BZ system can exhibit a vast array of NLD phenomena depending on the experimental conditions. Among them, chemical oscillations and chemical waves are the most studied. Chemical oscillations consist in the periodic variation of the concentration of catalyst and intermediates in the reaction medium. Such a variation is often manifested by a consequent variation in solution color (*e.g*. from yellow to colorless in the case of cerium catalyzed BZ systems) as well as electric potential.

Many recent studies are aimed at developing practical applications that benefit from exploiting NLD phenomena. Materials science and polymeric systems, in particular, seem to be a very promising field of application.[4,5] For example, by combining nonlinear chemical systems such as the BZ reaction, with polymerization reactions, it is possible to obtain either new materials or new synthetic ways for known materials.[6] This last strategy has already been proven to be viable in the case of the radical polymerization of poly-(acrylonitrile) using the BZ system as a "pulsating" source of radical species.[7] Moreover, polymeric materials are widely used in the field of NLD as a component of the experimental setup to prevent the onset of convective motions or to physically alter the reaction environment. Recently, for example, poly(ethylenoxide) was used in a microemulsion environment, to prove that the origin of some peculiar none-quilibrium patterns, namely dashed waves and segmented spirals, was due to the clustering of water droplets.[8]

Surfactant aggregated systems are know to influence BZ reaction by selectively sequestering some of the key inter-mediates and/or by affecting the physical properties of the reaction medium.[9,10] As a consequence, they are able to alter BZ system influencing its dynamics and even acting as a bifurcation parameter switching on or off some of its behaviors (*e.g*. oscillatory or chaotic).[11] In our previous works we have considered the effect of several aggregated systems and non-ionic polymers on the BZ reaction,[11–17] and even though most of the surfactants were chemically inert, the non-ionic polymers were found to react with some of the BZ key intermediates. Intriguingly, these studies enabled us to determine the presence of new reacting radical species, which can be further exploited for the polymerization reaction.

In this paper, we focus our attention on the effects of the initial reactants' concentration on the oscillatory dynamics of a BZ reaction performed in the presence of a non-ionic polymer. Changes in the kinetics were also found to be dependent on the type and extent of the perturbation due to

Dipartimento di Chimica Fisica "F. Accascina", Università degli Studi di Palermo, Viale delle Scienze Ed.17, 90128, Palermo, Italy. E-mail: tliveri@unipa.it
† Present address: Dipartimento di Chimica e Fisica della Terra ed Applicazioni alle Georisorse ed ai Rischi Naturali, Universit deli Studi di Palermo, *via* Archirafi 36, 90123 Palermo, Italy.
‡ Present address: Dipartimento di Chimica Universit di Siena, Via della Diana 2, Siena, Italy and Polo Universitario Colle Val d'Elsa Viale Matteotti 15, Colle Val d'Elsa, Siena, Italy.

the self-assembling properties of the polymer. Understanding the reasons behind this effect may be of great importance for the application of NLD to the synthesis of new materials.

Experimental

Materials

$Ce(SO_4)_2{\cdot}4H_2O$ (Ce(IV), Fluka), malonic acid (MA, Fluka), sodium bromate (Fluka), sulfuric acid (Fluka), methanol (MeOH, Fluka), ethylene glycol (EG, Fluka), poly(ethylene glycol) with molecular weight 2000 g mol^{-1} (PEG, Fluka), poly(ethylene glycol) dimethylether with molecular weight 2000 g mol^{-1} (MPEG, Fluka), sodium sulfate (Fluka), acetone (Fluka) and Red Nile (RN, Sigma) were of commercial analytical quality and were used without further purification.

Stock solutions of all chemicals used were prepared by weight before use. Stock solutions of sulfuric acid were standardized by acid–base titration. Deionized water from reverse osmosis (Elga, model Option 3), having resistivity higher than 1 MΩ cm, was used to prepare all solutions.

Kinetics measurements

All the kinetic measurements have been conducted with a computer-controlled Beckman model DU-640 UV-vis spectrophotometer, equipped with thermostatted compartments for 1 × 1 × 5 cm quartz cells and a magnetic stirring apparatus. The temperature of all the experiments was kept at 25.0 ± 0.1 °C with a thermostat HAAKE model D8.

Oscillating reactions

The oscillating mixtures for the kinetic runs were prepared by mixing aqueous stock solutions of $NaBrO_3$, Ce(IV) in 1.80 mol dm^{-3} sulfuric acid, MA in 1.80 mol dm^{-3} sulfuric acid and additive (at the desired concentration). Appropriate aliquots of the stock solutions were mixed in a 3 mL UV quartz cell in order to obtain the appropriate initial concentrations of reactants. The reaction was initiated by the addition of the Ce(IV) to the solution. The dynamics of the BZ system was followed in batch conditions, by monitoring the Ce(IV) absorbance at the appropriate wavelength, depending on the Ce(IV) concentration, in the range 350–450 nm. Reactive solutions were vigorously stirred to ensure homogeneity even for systems with high viscosity. The absorbance of Ce(IV) in the concentration range considered has been found to follow Lambert-Beer law for all the wavelengths used.

Being the experiment conducted in batch conditions, the concentration of the reagents will decrease with time leading to a drift in the oscillation period or an interruption of oscillations while the system approaches thermodynamic equilibrium. Nevertheless, the route toward the equilibrium is slow enough to make it possible to observe the BZ dynamics for a sufficient period of time. Consequently, the period of an oscillation has been calculated as the mean value of the first five oscillation cycles. Additionally, the induction period has been calculated as the time passed from the start of the reaction by the addition of the catalyst till the beginning of the first oscillation. All the oscillatory parameters values reported in this work are the mean of five different experiments.

Reaction of ethylene glycol with acidic bromate

Solutions were prepared directly in the spectrophotometric cell adding 0.6 mL H_2O + 0.6 mL 4.5 mol dm^{-3} H_2SO_4 + 1.5 mL 0.6 mol dm^{-3} $NaBrO_3$ + 0.3 mL 0.1 mol dm^{-3} ethylene glycol. The kinetics of the reaction has been followed by monitoring the absorbance of HOBr (produced in the course of the reaction) at 330 nm.

Viscosity measurements

The viscosity of PEG aqueous solutions was determined in the presence of 0.9 mol dm^{-3} H_2SO_4 and 0.03 mol dm^{-3} Na_2SO_4.

The relative viscosity (η_{rel}) of the aqueous polymer solutions was calculated from the well-known relationship

$$\eta_{rel} = \frac{t}{t_0}\frac{\rho}{\rho_0} \quad (1)$$

The solution flowing time (t) was measured with a Ostwald glass viscosimeter (id 0.46 mm and capillary length 9 cm) calibrated by measuring the solvent draining time (t_0), in our case an aqueous 0.90 mol dm^{-3} H_2SO_4 and 0.03 mol dm^{-3} Na_2SO_4 solution. The flowing time of the solvent in the glass capillary was 316.39 s.

Since in our experimental conditions, extremely dilute and dilute polymer solutions are used, the density correction has been reasonably ignored. Moreover, since the draining times of both the solvent and the solution are much longer than 100 s and a sufficiently high length/diameter ratio is reached, the kinetic energy corrections and end-effects were also neglected. Thus, the relative viscosity has been calculated as[18]

$$\eta_{rel} = \frac{t}{t_0} \quad (2)$$

The measurements were performed at 25.0 ± 0.1 °C using a stopwatch with an accuracy of 0.01 s.

All measurements were replicated three times and were reproducible to within one part per thousand. After measuring each PEG solution draining time the efflux time of the solvent has been determined again. The constancy of the solvent efflux time has been taken as a criterion for judging the consistency of experimental conditions and the state of the viscometer.

Fluorescence measurements

The steady-state Nile Red (NR) fluorescence spectra of PEG aqueous solution were registered with a Fluoromax 4 (Jobin-Yvon) spectrofluorometer (right angle geometry, 1 × 1 × 5 cm quartz cell) at 25.0 ± 0.1 °C. The excitation wavelength was of 490 nm and the emission spectra were recorded from 550 to 800 nm. The widths of the slits were set at 2 and 1 nm for excitation and emission, respectively. The NR aqueous solutions have been prepared accordingly to the procedure described elsewhere.[19]

Computer simulations

Simulations of the perturbation of the BZ system by the additives have been conducted using the Copasi kinetics

simulation software[20] by applying a modified MBM (Marburg-Budapest-Missoula) model mechanism.[21]

Results and discussion

In the experimental conditions used, the BZ system presents an induction period (IP) where the Ce(IV) concentration initially decreases and then remains nearly constant, followed by an oscillatory period, where the Ce(IV) concentration (as well as that of other intermediates) oscillates regularly with a time period τ and the amplitude A.

In the considered concentration range, the presence of PEG does not influence qualitatively the dynamics of the system. However, all the oscillation parameters (IP, τ and A) are quantitatively affected. In a previous work[13] we reported that the nature and the extent of this effect depend on the concentration of PEG in the mixture. In particular, it resulted in a decrease of IP at low concentration and in an increase of IP at high concentration while it induced a decrease of τ and A at any concentration considered. However, we successively noticed that the above mentioned effect may depend on the initial conditions of the BZ system. In fact, not only the oscillation parameters IP and τ change, but also the effect that PEG exerts on them may be completely different.

Fig. 1A–C shows the observed effects of the [PEG] on the IP at different concentrations of two of the key components of the BZ reaction, namely the catalyst, Ce(IV), and the oxidant, BrO_3^-. It can be noted that by increasing the Ce(IV) concentration, there is an inversion of the trend. In fact, at low [Ce(IV)] (Fig. 1a) the IP decreases and then increases on increasing PEG concentration, similarly to what has previously been reported.[13] At intermediate and higher [Ce(IV)] the IP increases for very low values of [PEG] and then decreases (Fig. 1B,C). Also the bromate concentration seems to play a role in modifying the effect of PEG perturbation even if it seems to be less relevant. Fig. 1A shows that, while the effect of PEG decreases in intensity on increasing the bromate concentration, the trends observed still remain the same. This is true also at medium Ce(IV) concentration (Fig. 1B). When the concentration of Ce(IV) increases, the system cannot sustain oscillatory behavior for lower bromate concentrations (Fig. 1–3 B,C). A similar effect has been observed also in the case of the oscillation period, τ. Fig. 2 shows that for low and intermediate [Ce(IV)] values (Fig. 2A,B) the trend observed is the same as previously reported, while at higher concentration (Fig. 2C) a slight increase in τ can be noted for low PEG concentrations. However, at higher PEG concentration τ values begin to decrease as well. Finally, as for the amplitude A, it has been observed that the polymer effect is negligible at low [PEG] for high and intermediate catalyst concentration (Fig. 3A,B) while at high [PEG] A starts to decrease. As for the higher [Ce(IV)], A always decreases with [PEG].

The different effects manifested at low and high PEG concentration can be explained taking into account the two-fold chemical nature of the polymer. In fact, the presence of the OH terminal group and of the polyether backbone perturbs differently the BZ system altering different reaction paths in the complex BZ mechanism. This scenario is

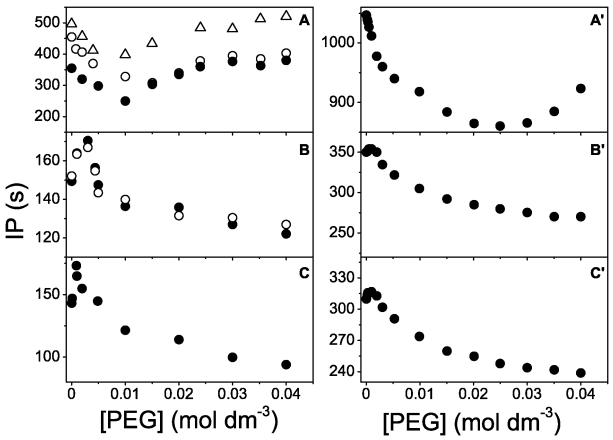

Fig. 1 Experimental (A, B, C) and simulated (A′, B′, C′) induction period values as a function of [PEG] for the perturbed BZ system. $[Ce(IV)]_0$ = (A,A′) 8.0×10^{-4} mol dm^{-3}, (B,B′) 5.0×10^{-3} mol dm^{-3}, (C,C′) 7.0×10^{-3} mol dm^{-3}; $[BrO_3^-]_0 = 7.5 \times 10^{-2}$ mol dm^{-3} (●), $[BrO_3^-]_0 = 4.0 \times 10^{-2}$ mol dm^{-3} (○), $[BrO_3^-]_0 = 3.0 \times 10^{-2}$ mol dm^{-3} (△); $[MA]_0 = 0.1$ mol dm^{-3}; $[H_2SO_4]_0 = 0.9$ mol dm^{-3}; $t = 25.0 \pm 0.1$ °C.

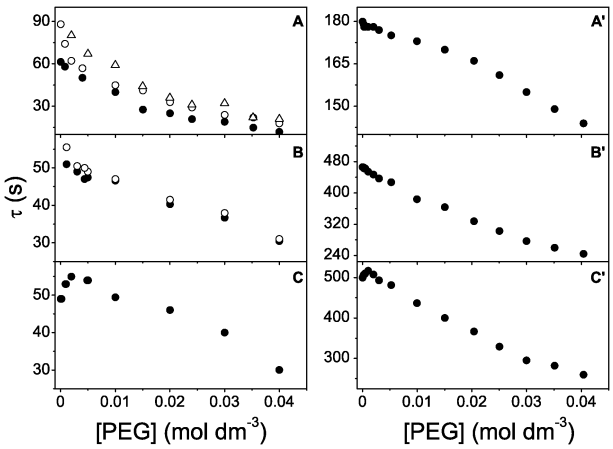

Fig. 2 Experimental (A, B, C) and simulated (A′, B′, C′) oscillation period values as a function of [PEG] for the perturbed BZ system. $[Ce(IV)]_0$ = (A,A′) 8.0×10^{-4} mol dm^{-3}, (B,B′) 5.0×10^{-3} mol dm^{-3}, (C,C′) 7.0×10^{-3} mol dm^{-3}; $[BrO_3^-]_0 = 7.5 \times 10^{-2}$ mol dm^{-3} (●), $[BrO_3^-]_0 = 4.0 \times 10^{-2}$ mol dm^{-3} (○), $[BrO_3^-]_0 = 3.0 \times 10^{-2}$ mol dm^{-3} (△); $[MA]_0 = 0.1$ mol dm^{-3}; $[H_2SO_4]_0 = 0.9$ mol dm^{-3}; $t = 25.0 \pm 0.1$ °C.

corroborated by experiments conducted using perturbing species featuring only one of the two reacting groups. Fig. 4 illustrates the effects of the presence of methanol, ethylene glycol and poly(ethylene glycol) dimethylether (MPEG) on the oscillation parameters of the perturbed BZ system. It can be noted that, under the experimental conditions reported in Fig. 4, the presence of an alcohol leads to a decrease of the IP (Fig. 4A,B) while the presence of MPEG leads to an increase of IP followed by a slight decrease at higher concentrations (Fig. 4C). Similar trends have been observed even in the case of τ (Fig. 4D–F) and in the case of A (Fig. 4G–I), except for the MPEG effect which is negligible. Therefore, in order to understand the global effect of PEG, we propose the

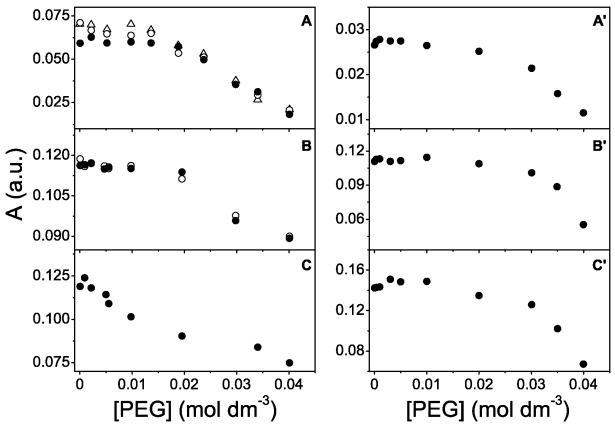

Fig. 3 Experimental (A, B, C) and simulated (A′, B′, C′) oscillation period values as a function of [PEG] for the perturbed BZ system. $[Ce(IV)]_0$ = (A,A′) 8.0×10^{-4} mol dm^{-3}, (B,B′) 5.0×10^{-3} mol dm^{-3}, (C,C′) 7.0×10^{-3} mol dm^{-3}; $[BrO_3^-]_0 = 7.5 \times 10^{-2}$ mol dm^{-3} (●), $[BrO_3^-]_0 = 4.0 \times 10^{-2}$ mol dm^{-3} (○), $[BrO_3^-]_0 = 3.0 \times 10^{-2}$ mol dm^{-3} (△); $[MA]_0 = 0.1$ mol dm^{-3}; $[H_2SO_4]_0 = 0.9$ mol dm^{-3}; $t = 25.0 \pm 0.1$ °C.

following mechanism which takes into account the twofold nature of the polymer.

Reactions of the terminal hydroxyl groups

The reaction of bromate with the hydroxyl groups produces bromous acid *via* the processes[13]

$$P - CH_2 - OH + BrO_3^- + H^+ \rightarrow P - CHO + HBrO_2 + H_2O \quad (R1)$$

$$P - CHO + BrO_3^- + H^+ \rightarrow P - COOH + HBrO_2 + H_2O \quad (R2)$$

Bromous acid produced in these reactions will participate in two different reaction pathways as described by the MBM mechanism. The first one is the autocatalytic cycle that re-oxidizes the catalyst

$$BrO_3^- + HBrO_2 + H^+ \rightarrow Br_2O_4 + H_2O \quad (MBM6)$$

$$Br_2O_4 \rightarrow 2BrO_2^\bullet \quad (MBM7)$$

$$BrO_2^\bullet + Ce(III) + H^+ \rightarrow Ce(IV) + HBrO_2 \quad (MBM8)$$

the other one is the formation of hypobromous acid by the reaction with bromide ion

$$HBrO_2 + Br^- \rightarrow 2HOBr \quad (MBM2)$$

the effects that these two reaction pathways would have on the IP are opposite. $BrO_2^\bullet$ is the autocatalytic species that is crucial for the positive feedback loop. An increase in its concentration would lead to an enhancement of the loop itself, which would mean an increase in the IP length. In fact, the induction period stops when the positive feedback loop is interrupted. On the other hand, the overproduction of HOBr would promote the bromination of malonic acid *via* the following reaction

$$HOBr + MA + H^+ \rightarrow BrMA + H_2O \quad (MBM31)$$

Bromomalonic acid is part of the negative feedback loop because its accumulation will promote the switching off of the positive feedback loop. Moreover, it is also possible that the reaction of HOBr with bromide would produce bromine that, in turn, would also produce bromomalonic acid.

$$HOBr + Br^- + H^+ \rightarrow Br_2 + H_2O \quad (MBM1)$$

$$MA(enol) + Br_2 \rightarrow BrMA + Br^- + H^+ \quad (MBM30)$$

Experimental results suggest that at high Ce(IV) concentration the pathway which leads to the production of HOBr predominates while the pathway involving reactions (MBM6) and (MBM7) will be more important at lower Ce(IV) concentrations.

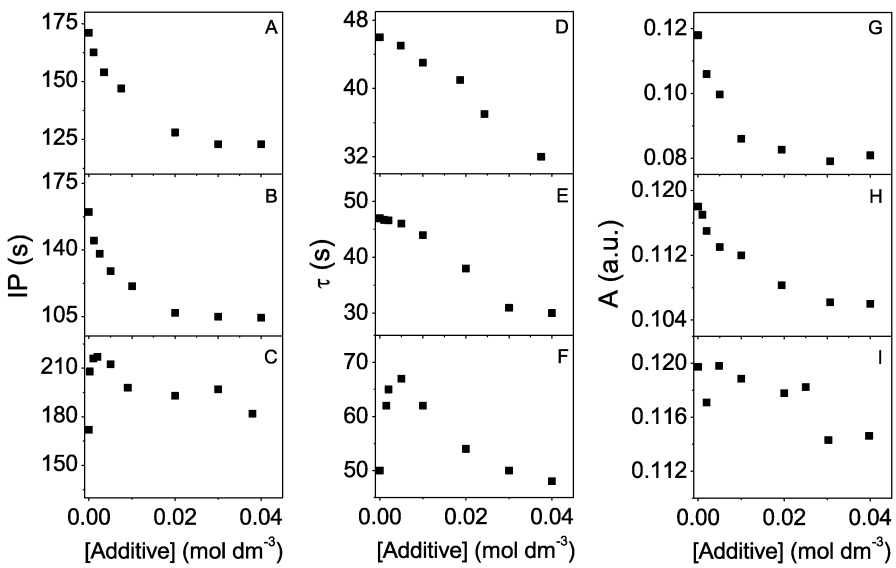

Fig. 4 Effect of single functional groups on the induction period (A–C), oscillation period (D–F) and oscillation amplitude (G–I) of the perturbed BZ system. (A, D, G) MeOH, (B, E, H) EG, (C, F, I) MPEG. $[MA]_0 = 0.1$ mol dm^{-3}; $[BrO_3^-]_0 = 7.5 \times 10^{-2}$ mol dm^{-3}; $[Ce(IV)]_0 = 7.0 \times 10^{-3}$ mol dm^{-3}; $[H_2SO_4]_0 = 0.9$ mol dm^{-3}; $t = 25.0 \pm 0.1$ °C.

This behavior can be rationalized by considering that the higher concentration of the catalyst enhances the production of the malonyl radical that reacts with the bromate

$$Ce(IV) + MA \rightarrow MA^{\bullet} + Ce(III) + H^{+} \quad (MBM27)$$

$$MA^{\bullet} + BrO_3^- + H^+ \rightarrow BrO_2^{\bullet} + TA \quad (MBM48)$$

This would hamper the reaction of the positive feedback loop involving the bromate instead of favoring the production of HOBr through reaction (MBM2). Moreover, the $BrO_2^{\bullet}$ radical is rapidly scavenged by the malonyl radical itself

$$MA^{\bullet} + BrO_2^{\bullet} \rightarrow BrO_2MA \quad (MBM32)$$

at lower Ce(IV) concentration reaction (MBM48) would not be very important and most of the bromate would be consumed *via* reactions (MBM6) and (MBM7).

The proposed mechanism is also able to simultaneously explain the decrease of the time period and of the amplitude both at high and low Ce(IV) concentrations. In fact, at high concentration of the catalyst the larger production of HOBr accelerates the production of bromomalonc acid resulting in a smaller time period and amplitude of the oscillations. A similar effect is observed also at low Ce(IV) concentration. This can be explained taking into account that the inflow of the autocatalytic intermediate $BrO_2^{\bullet}$ would result in a longer autocatalytic phase and a shorter inhibitory one. As in the present BZ system the inhibitory phase is much longer than the autocatalytic one, the resulting effect is a decrease of the total time period and amplitude of the oscillation.

Reactions of the polyether chain

Explanation for the observed effects on the oscillatory parameters are also provided by the knowledge that Ce(IV) reacts with the PEG according to[22,23]

$$Ce(IV) + PEG \rightarrow Ce(III) + PEG^{\bullet} + H^{+} \quad (R3)$$

Moreover, it has been found[24,25] that Ce(IV) can also react with the PEG radicals through the following reaction of oxidative termination

$$Ce(IV) + PEG^{\bullet} \rightarrow Ce(III) + P + H^{+} \quad (R4)$$

where P stands for *polymer*. In addition, a reaction analogous to (R3), involving $BrO_2^{\bullet}$ radical has also been previously proposed[13]

$$BrO_2^{\bullet} + PEG \rightarrow HBrO_2 + PEG^{\bullet} \quad (R5)$$

The formed PEG radicals can thus scavenge the $BrO_2^{\bullet}$ and the product may subsequently decompose *via* two possible pathways

$$BrO_2^{\bullet} + PEG^{\bullet} \rightarrow BrO_2 - PEG \quad (R6)$$

$$BrO_2 - PEG \rightarrow P1 + HOBr \quad (R7)$$

$$BrO_2 - PEG \rightarrow P2 + HBrO_2 \quad (R8)$$

where P1 and P2 are nonreactive products. Previous results showed that reaction (R7) dominates on (R8) leading to an increase of HOBr in the systems. Moreover, another reaction, involving the bromine specie can also be proposed

$$Br_2 + PEG \rightarrow Br^- + BrPEG + H^+ \quad (R9)$$

reaction (R9) is the result of the following processes, recently proposed by Nagy-Ungvaray et co-workers[26]

$$Br_2 \rightarrow 2Br^{\bullet} \quad (R10)$$

$$Br^{\bullet} + P - OH \rightarrow P^{\bullet} - OH + Br^- + H^+ \quad (R11)$$

and the recombination of the two radicals:

$$Br^{\bullet} + P^{\bullet} - OH \rightarrow Br - P - OH \quad (R12)$$

The effects of all these reactions can be summarized as follows:

- Reactions (R5)–(R8) would remove $BrO_2^{\bullet}$ radical from the system and, at the same time, increase the amount of HOBr leading to reduction of all the oscillatory parameters.
- The decrease of bromine, due to reaction (R9), would lead to an increase of IP due to the fact that the production of BrMA by reaction (MBM30) would be hampered. Consequently, a longer time would be needed for the critical amount of BrMA to accumulate in the system and switch off the autocatalytic cycle. For the same reason, the time period would also be longer, due to the fact that a longer time would be required for turning on the autocatalytic phase again.

It is possible to explain the difference of PEG effects on changing Ce(IV) concentration by taking into account the role played by the catalyst in the unperturbed BZ systems. In fact, it can be reasonably proposed that the concentration of bromine will be higher at high Ce (IV) concentration due to its production *via* reaction (MBM1) while the concentration of the autocatalytic intermediate $BrO_2^{\bullet}$ will be lower because of its scavenging by malonyl radicals. As a consequence, the contribution of reactions (R5)–(R8) is negligible at low PEG concentration and starts to become important only at higher polymer concentration. When the concentration of Ce(IV) is lower, there will be higher availability of $BrO_2^{\bullet}$ and a lower concentration of bromine, therefore, the effect of reactions (R5)–(R8) always dominates.

Model simulation

To simulate the response of the BZ system for polymer perturbation, the reactions proposed in the previous sections for the terminal groups and for the backbone have been introduced into the full MBM mechanism (48 reactions, 35 chemical species). As already observed in our previous work,[13] the model thus modified is able to reproduce the separate perturbations due to alcoholic end-groups and the polyether backbones, but proved unsuccessful in reproducing the experimental behavior reported in Fig. 1–3. We then considered the possibility that the global perturbation of the PEG could be ascribed not only to the twofold nature of the polymer but also to some peculiar physicochemical properties of the PEG aqueous solutions. The latter were investigated by performing systematic viscosimetric and spectrofluorimetric measurements, the results of which will be discussed in the following subsections.

Viscosimetric data. The complete course of the relative viscosity (η_{rel}) as a function of non-ionic polymer concentration is shown in Fig. 5A. It has to be mentioned that both the

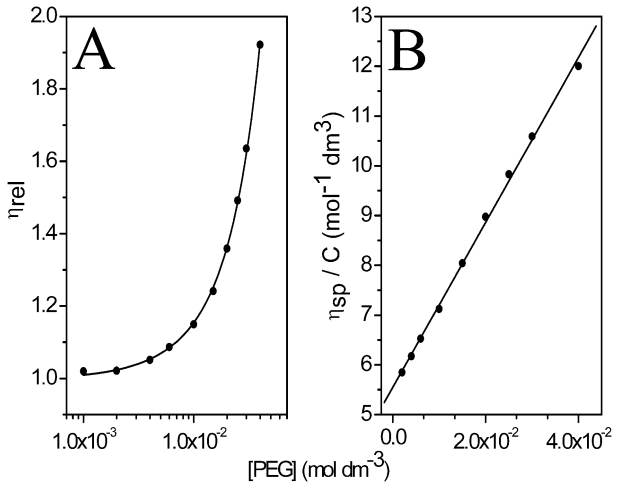

Fig. 5 (A) Relative viscosity of aqueous polymer solution as a function of PEG concentration in the presence of 0.90 mol dm^{-3} H_2SO_4 and 0.03 mol dm^{-3} Na_2SO_4, $t = 25.0 \pm 0.1$ °C, (—) guide for the eyes; (B) Reduced viscosity of aqueous polymer solution as a function of PEG concentration in the presence of 0.90 mol dm^{-3} H_2SO_4 and 0.03 mol dm^{-3} Na_2SO_4, $t = 25.0 \pm 0.1$ °C, (—) linear fit to eqn (4).

shape and the viscosity enhancement obtained in our work in the presence of electrolyte are very close to those reported in the literature for pure water.[27] This implies that the presence of electrolytes does not influence the polymer behavior as has to be expected for a non-ionic polymer.

Perusal of the figure reveals that the relative viscosity does not depend linearly on the [PEG]. This means that the Einstein viscosity law ($\eta_{rel} = 1 + [\eta]C$, where C is the PEG concentration and $[\eta]$ is the intrinsic viscosity) proposed for non-interacting polymer chains in dilute solution is not valid. Thus, the deviation for linearity has been explained in the light of the theoretical approach[28–30] based on the concept of self-association or cluster formation in dilute polymer solution. In particular, in the early 1950s[31–33] it has been proposed that there exists a boundary concentration which separates a dilute polymer solution into two regions. This concentration has been named by Qian[34–36] "dynamic contact concentration", C_s. At this concentration the chain segments of a polymer coil start to "feel" repulsive forces due to the interaction with the segments of the neighboring coils. Because of the dynamic contact during molecular motion, when the polymer concentration C is higher than C_s, the coils undergo a conformational change and shrink in dimensions. The existence of the dynamic contact concentration has been widely proved both experimentally and theoretically.[30,37–43]

According to the model described in ref. 28–30, the aggregation of the polymer in solution can be described by multiple equilibria with an identical molar self-association constant K_a

$$P + P \overset{K_a}{\longleftrightarrow} P_2$$

$$P_2 + P \overset{K_a}{\longleftrightarrow} P_3$$

$$\ldots\ldots$$

$$P_{i-1} + P \overset{K_a}{\longleftrightarrow} P_i$$

Using the mass action law (with M being the molar mass polymer) K_a is related to the "apparent association constant for monodispersed polymer chains in solution", K_m, by the equation

$$K_m = \frac{K_a}{M} \quad (3)$$

This constant is related to the reduced viscosity, η_{red} ($\eta_{red} = \eta_{sp}/C$, where $\eta_{sp} = \eta_{rel} - 1$) by eqn (4)

$$\eta_{red} = [\eta] + 6\ K_m[\eta]C \quad (4)$$

and to the dynamic contact concentration C_s by eqn (5)

$$C_s = \frac{0.001}{2K_m} \quad (5)$$

We have calculated the reduced viscosity (η_{red}) of the PEG aqueous solutions and the results are shown in Fig. 5B. A linear trend has been found and the linear least-squares analysis of the data yields the values of $[\eta] = 5.54 \pm 0.06$ dm^3 mol^{-1} and $K_m = 4.94 \pm 0.01$ mol dm^{-3}. Finally, by using eqn (4) the dynamic contact concentration C_s was found to be $(1.012 \pm 0.001) \times 10^{-4}$ mol dm^{-3}.

The obtained value for K_m is lower with respect to those reported by Cai *et al.*[43] while that for C_s is higher. The results are perfectly in line with the lower molecular weight of our PEG (2000 g mol^{-1}) with respect to their PEO (3.9×10^5 g mol^{-1}).

As for the $[\eta]$ value, it is lower with respect to that previously reported.[44] Since the $[\eta]$ represents the extrapolation of η_{sp}/[PEG] to zero solute concentration, it is evident that additional viscosity data in the very diluted region are needed. However, it is well known that the repeatability of the viscosimetric measurements in the extremely diluted region is very poor[12] due to various experimental problems. Thus, we obtained further evidence of the existence of the dynamic contact concentration by performing spectrofluorimetric measurements. In fact, fluorophore probes are very sensitive to the medium polarity.

Spectrofluorimetric data. The emission spectra of the NR in aqueous PEG solution have been monitored over a wide polymer concentration, *i.e.*, from the extremely diluted region to the dilute one. An interesting behavior has been observed. In particular, as shown in Fig. 6A in the PEG concentration range 0–3.0×10^{-4} mol dm^{-3} the profiles of the emission as a function of wavelength were substantially unchanged with respect to that in the absence of PEG. It is evident that neither the shape nor the maximum wavelength is affected by the presence of the non-ionic polymer. The emission spectrum obtained in the present work is similar to that reported in the literature[45] and has been well fitted by two Gaussian functions, the first having a maximum at 641 nm and the second one at 661 nm. The presence of the two peaks has been explained[45] by considering that the NR is almost insoluble in water and, as a consequence, aggregation of NR molecules takes place. These organized aggregates most likely affect the energy transfer process from one configurational state, corresponding to the band at 641 nm, to the other, corresponding to the band at 661 nm, giving rise to dual fluorescence.

As for the PEG concentration range 5.0×10^{-4}–4.0×10^{-2} mol dm^{-3}, it can be seen from Fig. 6B that both the shape

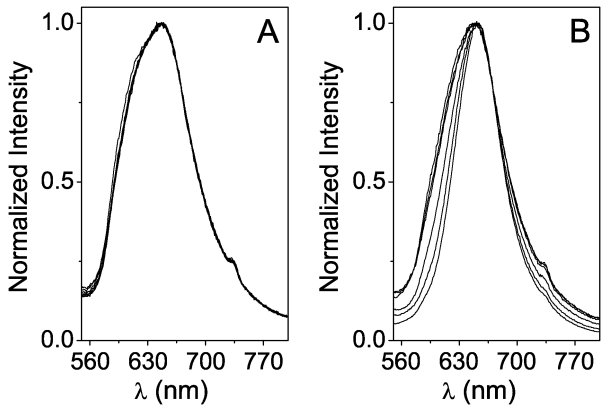

Fig. 6 Fluorescence spectra of 8.0×10^{-6} mol dm^{-3} NR in the presence of PEG in the concentration range (A) 0–3.0×10^{-4} mol dm^{-3} and (B) 5.0×10^{-4}–4.0×10^{-2} mol dm^{-3}, t = 25.0 ± 0.1 °C.

and the maximum wavelength significantly change. Particularly, the emission spectra were fitted by only one Gaussian and a blue shift of the λ_{max} was detected as a function of PEG concentration (see Fig. 7A). This implies that the NR probe experiences an environment with decreased polarity.

The presence of one peak clearly indicates that the NR interacts with the PEG to an extent that depends on the PEG concentration, and solubilization in the polymer coils occurs. In addition, the wavelength shift[46,47] has been correlated to the transition energies E_{NR} ($= 1.196 \times 10^5/\lambda_{max}$), It can be seen from Fig. 7B that the NR transition energies decrease on increasing the PEG concentration. The decrease of this parameter is correlated[45,47] with the decrease of the medium polarity.

It is worth to note that the PEG concentration at which the changes in the fluorescence spectrum happen is very close to the dynamic contact concentration C_s evaluated by means of the viscosimetric data. The small difference could be explained, by considering that the lack of viscosimetric data at low [PEG] does not allow a precise fitting. Moreover, it can be explained, analogously to the critical micelle concentration of aqueous surfactant solution, by considering that a different experimental method can give a diverse answer.

Viscosimetric and spectrofluorometric measurements demonstrated that for concentrations higher than C_s, PEG

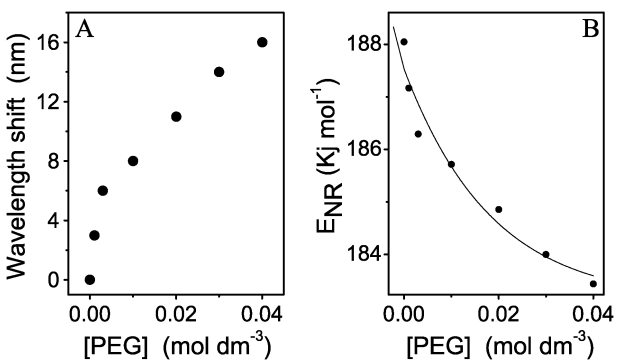

Fig. 7 (A) Maximum fluorescence wavelength shift of NR as a function of PEG concentration; (B) transition energy of Nile Red as a function of PEG concentration.

polymer exists in solution as a mixture of a random coil molecule and cluster chains. In the light of these results, simulations using the MBM mechanism[21] have been performed considering both single and aggregated PEG species. For each analytical concentration of the polymer, the initial concentration of the different species has been calculated on the basis of the K_a and K_m values determined through viscosimetric measurements.

However, we have considered only the formation of dimer species. This choice is justified by considering that, for instance, at PEG concentration of 0.01 mol dm^{-3} the monomer (PEG), dimers (PEG_2) and trimers (PEG_3) concentration in solution is 9.1×10^{-3} mol dm^{-3}, 4.0×10^{-4} mol dm^{-3} and 1.8×10^{-5} mol dm^{-3}, respectively, which correspond to a percentage of about 91.4, 8 and 0.55%, respectively. As a consequence, we have not taken into account the trimers concentration and all the terms above.

Simulations. The reactions involving the polymer used in the modified MBM model are reported in Table 1.

Note that, as for the monomeric form of PEG, the effect due to the OH terminal groups has been simulated by introducing reaction (R13), which is the result of reactions (R1) and (R2), and reaction (R14) for the second alcoholic terminal group, while, regarding the polymeric backbone perturbation, we introduced reactions (R3)–(R9) described in the previous sections.

At present, the exact values for the kinetic constant for these reactions are not known; however, kinetic measurements aimed at investigating the reactivity of PEG toward some key BZ components are in progress and will be the subject of a future publication. At this stage we applied some estimated values in order to see if the proposed mechanism was able to reproduce the obtained results.

As for the reactivity of alcoholic groups, it is reasonable to estimate the value of the rate constants for the oxidation of PEG, starting from experimental data relative to EG. Therefore, the kinetic constant for reaction (R13) has been chosen to be equal to the corresponding kinetic constant in the case of ethylene glycol. In particular, the latter has been calculated by measuring the absorbance of HOBr produced in the course of the reaction of ethylene glycol with acidic bromate, following the procedure reported in Pelle *et al.*[48] while for reaction (R14) an estimated value, lower than k_{13} has been used.[48]

Regarding the polymeric backbone reactions, we have chosen k_3 in light of the results of some kinetic measurements showing that the time scale of reaction (R3) is quite long in comparison with the time needed for the BZ system to reach the oscillatory phase, whereas for k_4 a much higher value has been used since reaction (R4) involves radical species. The value of k_5 has been chosen to be two orders of magnitude higher than that proposed in our previous work.[13] In fact, we found that the present value better fits the experimental data under the different experimental conditions studied. The same value has also been used for k_9 because reactions (R5) and (R9) show the same mechanism.[26] Finally, k_6 has been set to a high value by assuming that the rate determining step of the process (R6)–(R8) leading to HOBr and $HBrO_2$ is a diffusion controlled radical-radical recombination reaction.[13]

Table 1 Scheme of the perturbative reactions used in the simulations

	Reaction of the OH terminal group	
R13	$PEG + 2HBrO_3 \rightarrow HO–CH_2–P–COOH + 2HBrO_2 + 2H_2O$	$k_{13} = 3.5 \times 10^{-3}\ s^{-1}\ dm^9\ mol^{-2}$
R′13	$PEG_2 + 2HBrO_3 \rightarrow HO–CH_2–P_2–COOH + 2HBrO_2 + 2H_2O$	$k'_{13} = 2.0 \times 10^{-3}\ s^{-1}\ dm^9\ mol^{-2}$
R14	$HO–CH_2–P–COOH + 2HBrO_3 \rightarrow HOOC–P–COOH + 2HBrO_2 + 2H_2O$	$k_{14} = 1.0 \times 10^{-3}\ s^{-1}\ dm^9\ mol^{-2}$
R′14	$HO–CH_2–P_2–COOH + 2HBrO_3 \rightarrow HOOC–P_2–COOH + 2HBrO_2 + 2H_2O$	$k'_{14} = 5.0 \times 10^{-4}\ s^{-1}\ dm^9\ mol^{-2}$
	Reaction of the polymeric backbone	
R3	$Ce(IV) + PEG \rightarrow PEG^{\bullet} + Ce(III) + H^+$	$k_3 = 5.0 \times 10^{-3}\ dm^3\ mol^{-1}\ s^{-1}$
R′3	$Ce(IV) + PEG_2 \rightarrow PEG_2^{\bullet} + Ce(III) + H^+$	$k'_3 = 5.0 \times 10^{-4}\ dm^3\ mol^{-1}\ s^{-1}$
R4	$Ce(IV) + PEG^{\bullet} \rightarrow P + Ce(III) + H^+$	$k_4 = 1.0 \times 10^{3}\ dm^3\ mol^{-1}\ s^{-1}$
R′4	$Ce(IV) + PEG_2^{\bullet} \rightarrow P_2 + Ce(III) + H^+$	$k'_4 = 1.0 \times 10^{3}\ dm^3\ mol^{-1}\ s^{-1}$
R5	$PEG + BrO_2^{\bullet} \rightarrow PEG^{\bullet} + HBrO_2$	$k_5 = 4.0 \times 10^{5}\ dm^3\ mol^{-1}\ s^{-1}$
R′5	$PEG_2 + BrO_2^{\bullet} \rightarrow PEG_2^{\bullet} + HBrO_2$	$k'_5 = 1.0 \times 10^{2}\ dm^3\ mol^{-1}\ s^{-1}$
R6	$PEG^{\bullet} + BrO_2^{\bullet} \rightarrow PEGBrO_2$	$k_6 = 1.0 \times 10^{9}\ dm^3\ mol^{-1}\ s^{-1}$
R′6	$PEG_2^{\bullet} + BrO_2^{\bullet} \rightarrow PEGBrO_2$	$k'_6 = 1.0 \times 10^{9}\ dm^3\ mol^{-1}\ s^{-1}$
R7	$BrO_2–PEG \rightarrow P1 + HOBr$	$k_7 = 1.0 \times 10^{12}\ s^{-1}$
R′7	$BrO_2–PEG_2 \rightarrow P1 + HOBr$	$k'_7 = 1.0 \times 10^{12}\ s^{-1}$
R8	$BrO_2–PEG \rightarrow P2 + HBrO_2$	$k_8 = 1.0 \times 10^{12}\ s^{-1}$
R′8	$BrO_2–PEG_2 \rightarrow P2 + HBrO_2$	$k'_8 = 1.0 \times 10^{12}\ s^{-1}$
R9	$Br_2 + PEG \rightarrow BrPEG + H^+ + Br^-$	$k_9 = 4.0 \times 10^{5}\ dm^3\ mol^{-1}\ s^{-1}$
R′9	$Br_2 + PEG_2 \rightarrow BrPEG_2 + H^+ + Br^-$	$k'_9 = 1.0 \times 10^{2}\ dm^3\ mol^{-1}\ s^{-1}$

As for the aggregated form of the polymer, we assumed that dimers participate in the same perturbative reactions as the monomers. However, since the chain-to-chain interactions force the polymer chain to shrink, the polyether backbones result in being less available and therefore less reactive toward the BZ components, the rate constants of the processes involving the cluster chains have been chosen much lower than that involving the monomers. Moreover, by considering that in reactions R′4 and R′6 radical species (which always react very fast) are involved, reasonably we did not change the rate constant values with respect to the corresponding (R4) and (R6).

Finally, the constants k'_{13} and k'_{14} have been slightly reduced with respect to k_{13} and k_{14}, by considering that the hetero-association of the PEG chains makes the alcoholic terminal groups less accessible for the reactions.

The perturbation effect obtained by applying the proposed model is shown in Fig. 1–3 for three different initial catalyst concentrations, *i.e.* the same values reported for experimental runs. It can be noticed that, in accordance with the experimental results, the effect of the presence of PEG strongly depends on the catalyst concentration and the simulation results agree well with the experimental data, under all the experimental conditions investigated.

Conclusions

The perturbation induced by a polymeric material in a non linear chemical system, such as the BZ reaction, may depend on many factors including the concentration of the BZ components, the chemical nature of the polymer, its concentration and the physicochemical properties of its aqueous solution. As a consequence, the effects of the perturbation are a combination of such factors which, due to the non linearity of the systems involved, may lead to very different results. In recent works[49–53] it was pointed out how the combination of self-assembling processes, typical of equilibrium systems, with the self-organizing properties typical of dissipative systems, generally brings about the emergence of new and unpredictable behaviors. In this perspective, we have described and simulated a synergistic effect due to the changes in the initial reactants concentration of the BZ reaction combined with the aggregation properties typical of surfactants and polymers. These aspects have to be taken into account in many possible applications of NLD to polymeric systems. The simulation of the BZ system with the MBM mechanism provided results that qualitatively agree with the experimental data. This corroborates the proposed perturbation mechanism and also confirms the robustness of the MBM mechanism in very different conditions and in the presence of external perturbation. Consequently, model simulations could prove very helpful in applications development. Nevertheless, there is still quantitative disagreement with experimental results. This suggests that better estimates of the kinetic constant values are needed. Moreover, the MBM itself would probably need to be modified at some point to achieve better agreement.

Acknowledgements

The authors thank the Università degli Studi di Palermo for financial support (Research Funds ex quota 60%). F.R. was supported by a Marie Curie International Outgoing Fellowship within the 7th European Community Framework Programme. We would like to thank the "*Fondazione Banco di Sicilia*" (Palermo, Italy) which co-financed the Fluoromax 4 (Jobin-Yvon) spectrofluorometer (Convenzione PR19.b/06). Thanks are also due to Mr Casimiro Caruso (University of Palermo) for experimental help.

References

1 B. P. Belousov, in *Sbornik Referatov po Radiatsonno Meditsine*, Medgiz, Moscow, 1958, pp. 145–147.
2 A. M. Zhabotinsky, *Proc. Acad. Sci. USSR*, 1964, **157**, 392–395.
3 A. F. Taylor, *Prog. React. Kinet. Mech.*, 2002, **27**, 247–325.
4 I. R. Epstein and J. A. Pojman, *Chaos*, 1999, **9**, 255–259.

5 J. Pojman, *Macromol. Symp.*, 2000, **160**, 207–214.
6 J. A. Pojman, D. C. Leard and W. West, *J. Am. Chem. Soc.*, 1992, **114**, 8298–8299.
7 R. P. Washington, W. W. West, G. P. Misra and J. A. Pojman, *J. Am. Chem. Soc.*, 1999, **121**, 7373–7380.
8 J. Carballido-Landeira, I. Berenstein, P. Taboada, V. Mosquera, V. Vanag, I. Epstein, V. Perez-Villar and A. Munuzuri, *Phys. Chem. Chem. Phys.*, 2008, **10**, 1094–1096.
9 A. Paul, *J. Phys. Chem. B*, 2005, **109**, 9639–9644.
10 F. Rossi, R. Lombardo, L. Sciascia, C. Sbriziolo and M. L. T. Liveri, *J. Phys. Chem. B*, 2008, **112**, 7244–7250.
11 M. Rustici, R. Lombardo, M. Mangone, C. Sbriziolo, V. Zambrano and M. L. T. Liveri, *Faraday Discuss.*, 2002, **120**, 39–51.
12 F. Cavasino, R. Cervellati, R. Lombardo and M. Turco Liveri, *J. Phys. Chem. B*, 1999, **103**, 4285–4291.
13 R. Lombardo, C. Sbriziolo, M. L. T. Liveri, K. Pelle, M. Wittmann and Z. Noszticzius, in *Nonlinear Dynamics in Polymeric Systems*, ed. J. A. Pojman and Q. Tran-Cong-Miyata, Washington DC, 2004, vol. 869, pp. 292–308.
14 L. Sciascia, R. Lombardo and M. L. T. Liveri, *Chem. Phys. Lett.*, 2006, **430**, 67–70.
15 L. Sciascia, R. Lombardo and M. L. Turco Liveri, *J. Phys. Chem. B*, 2007, **111**, 1354–1360.
16 F. Rossi, R. Varsalona and M. L. T. Liveri, *Chem. Phys. Lett.*, 2008, **463**, 378–382.
17 R. Lombardo, F. Rossi, C. Sbriziolo, L. Sciascia and M. Liveri, in *American Chemical Society, Polymer Preprints, Division of Polymer Chemistry*, 2008, vol. 49, pp. 751–752.
18 D. Du, J. Zuo, Y. An, L. Zhou and Y. Liu, *J. Appl. Polym. Sci.*, 2006, **102**, 4440–4446.
19 S. Hassoon and I. Schechter, *Anal. Chim. Acta*, 1998, **368**, 77–82.
20 http://www.copasi.org/tiki-index.php?page=homepage.
21 L. Hegedus, M. Wittmann, Z. Noszticzius, S. H. Yan, A. Sirimungkala, H. D. Forsterling and R. J. Field, *Faraday Discuss.*, 2002, **120**, 21–38.
22 G. Odian, *Principles of Polymerization*, Wiley & Sons, New York, US, 3rd edn, 1991.
23 J. M. Harris, *Poly(ethylene Glycol) Chemistry: biotechnical and biomedical applications*, Plenum Press, New York and London, 1992.
24 T. Ozturk and I. Cakmak, *I. Polym. J.*, 2007, **16**, 561–581.
25 M. Degirmenci, S. Hicri and H. Yilmaz, *Eur. Polym. J.*, 2008, **44**, 3776–3781.
26 P. I. Kumli, M. Burger, M. J. B. Hauser, S. C. Muller and Z. Nagy-Ungvarai, *Phys. Chem. Chem. Phys.*, 2003, **5**, 5454–5458.
27 C. Branca, S. Magazu, G. Maisano, F. Migliardo, P. Migliardo and G. Romeo, *J. Phys. Chem. B*, 2002, **106**, 10272–10276.
28 R. S. Cheng, *Polymers and Organic Solids*, Science Press, Beijing, 1997.
29 M. Liu, R. Cheng, C. Wu and R. Qian, *J. Polym. Sci., Part B: Polym. Phys.*, 1997, **35**, 2421–2427.
30 Y. Pan and R. S. Cheng, *Chin. J. Polym. Sci.*, 2000, **18**, 57.
31 R. F. Boyer and R. S. Spencer, *J. Polym. Sci.*, 1950, **5**, 375–378.
32 D. J. Streeter and R. F. Boyer, *J. Polym. Sci.*, 1954, **14**, 5–14.
33 D. C. Pepper and P. P. Rutherford, *J. Polym. Sci.*, 1959, **35**, 299–301.
34 R. Qian, Pergamon Press, Oxford, UK, 1982, p. 139.
35 R. Qian, T. Cao, S. Chen and F. Bai, *Science in China Series B*, 1983, **12**, 1080.
36 R. Qian, *Perspectives on the macromolecular condensed state*, World Scientific, Singapore, 2002.
37 A. Dondos and D. Papanagopoulos, *Makromol. Chem. Rapid Commun.*, 1993, **14**, 7–11.
38 A. Dondos and D. Papanagopoulos, *Polymer*, 1995, **36**, 365–368.
39 D. Papanagopoulos and A. Dondos, *Macromol. Chem. Phys.*, 1994, **195**, 439–448.
40 D. Papanagopoulos and A. Dondos, *Polymer*, 1996, **37**, 1053–1055.
41 M. Liu, R. Cheng and R. Qian, *J. Polym. Sci., Part B: Polym. Phys.*, 1995, **33**, 1731–1735.
42 C. Wu, *J. Polym. Sci., Part B: Polym. Phys.*, 1994, **32**, 1503–1509.
43 J. Cai, S. Bo and R. Cheng, *Colloid Polym. Sci.*, 2003, **282**, 182–187.
44 C. Branca, S. Magazù, G. Maisano, P. Migliardo, F. Migliardo and G. Romeo, *Phys. Scr.*, 2002, **66**, 175–179.
45 A. K. Dutta, K. Kamada and K. Ohta, *J. Photochem. Photobiol., A*, 1996, **93**, 57–64.
46 P. Kipkemboi and A. Easteal, *Aust. J. Chem.*, 1994, **47**, 1771–1781.
47 F. D'Anna, V. Frenna, S. La Marca, R. Noto, V. Pace and D. Spinelli, *Tetrahedron*, 2008, **64**, 672–680.
48 K. Pelle, M. Wittmann, Z. Noszticzius, R. Lombardo, C. Sbriziolo and M. L. Turco Liveri, *J. Phys. Chem. A*, 2003, **107**, 2039–2047.
49 T. Yamaguchi, N. Suematsu and H. Mahara, in *Nonlinear Dynamics in Polymeric Systems*, ed. J. A. Pojman and Q. Tran-Cong-Miyata, Washington DC, 2004, vol. 869, pp. 16–27.
50 I. R. Epstein and V. K. Vanag, *Chaos*, 2005, **15**, 047510–047517.
51 F. Rossi, S. Ristori, M. Rustici, N. Marchettini and E. Tiezzi, *J. Theor. Biol.*, 2008, **255**, 404–412.
52 F. Rossi and M. L. T. Liveri, *Ecol. Modell.*, 2009, **220**, 1857–1864.
53 A. S. Mikhailov and G. Ertl, *ChemPhysChem*, 2009, **10**, 86–100.

